Analyst

Accepted Manuscript

ROYAL SOCIETY OF CHEMISTRY

www.rsc.org/analyst

[Preparation for publication as a paper in *Analyst*]

Ag@SiO_2-entrapped hydrogel microarray: A new platform for a metal-enhanced fluorescence-based protein assay

Eunji Jang[+], Minsu Kim[+] and Won-Gun Koh [*]

Department of Chemical and Biomolecular Engineering, Yonsei University

50 Yonsei-ro, Seodaemun-gu, Seoul 120-749, South Korea

[+] Eunji Jang and Minsu Kim contributed equally to this work

*Author to whom correspondence should be addressed. Department of Chemical and Biomolecular Engineering, Yonsei University, 50 Yonsei-ro, Seodaemun-gu, Seoul 120-749, South Korea

E-mail: wongun@yonsei.ac.kr, Phone: 82-2-2123-5755, Fax: 82-2-312-6401

Abstract

We developed a novel protein-based bioassay platform utilizing metal-enhanced fluorescence (MEF), which is a hydrogel microarray entrapping silica-coated silver nanoparticles ($Ag@SiO_2$). As a model system, different concentrations of glucose were detected using a fluorescence method by sequential bienzymatic reaction of hydrogel-entrapped glucose oxidase (GOX) and peroxidase (POD) inside a hydrogel microarray. Microarrays based on poly(ethylene glycol)(PEG) hydrogels were prepared by photopatterning a solution containing PEG diacrylate (PEG-DA), photoinitiator, enzymes, and $Ag@SiO_2$. The resultant hydrogel microarrays were able to entrap both enzymes and $Ag@SiO_2$ without leaching and deactivation problems. The presence of $Ag@SiO_2$ within the hydrogel microarray enhanced the fluorescence signal, and the extent of the enhancement was dependent on the thickness of silica shells and the amount of $Ag@SiO_2$. Optimal MEF effects were achieved when the thickness of the silica shell was 17.5 nm and 0.5 mg/mL of $Ag@SiO_2$ was incorporated into the assay systems. Compared with the standard hydrogel microarray-based assay performed without $Ag@SiO_2$, more than a 4-fold fluorescence enhancement was observed in a glucose concentration range between 10^{-3} mM and 10.0 mM using hydrogel microarray entrapping $Ag@SiO_2$, which led to significant improvements in the sensitivity and the limit of detection (LOD). The hydrogel microarray system presented in this study could be successfully combined with a microfluidic device as an initial step to create an MEF-based micro-total-analysis-system (μ-TAS).

Keyword: Metal-enhanced fluorescence; Protein-based bioassay; Silica-coated silver nanoparticles; Hydrogel microarray; Microfluidic device

Introduction

After completion of the human genome project, the scientific community has turned its attention toward proteomics. With the thrust of scientific endeavor moving from genomics to proteomics, various protein-based assay platforms have been developed to analyze interactions between certain types of proteins, such as antibodies and enzymes, with other proteins, peptides, low-molecular weight compounds, oligosaccharides, and DNA.[1-3]

Many of the protein-based assays use fluorescence detection methods. Recently, the fluorescence detection method utilizing metal-enhanced fluorescence (MEF) has been widely studied in an effort to improve the detection sensitivity of protein-based bioassays.[4-7] MEF is now a well-established technology, wherein the interactions of fluorophores with metallic nanoparticles results in fluorescence enhancement. This phenomenon results from the combined effects of the creation of an intense excitation field around the metal nanoparticle in the vicinity of the fluorophore, an increase in the intrinsic emission rate of the fluorophore, and a strong coupling between the fluorophore and the plasmons in the metal.[8-11] Among various metals, silver nanostructures are the most commonly employed due to their intense surface plasmon resonance and ease of preparation. Two different silver platforms have been utilized for MEF-based biosensing. First, silver nanostructures were prepared on the two-dimensional (2D) flat substrates as silver island films (SIF) or 2D monolayers of silver nanoparticles (AgNPs) for metal-enhanced planar assays.[12-18] However, when biomolecules such as proteins are immobilized onto 2D substrates, the amount of protein that can be attached is limited, resulting in a relatively low sensitivity of the assay. Furthermore, immobilized proteins may dehydrate and denature due to the rapid evaporation of the liquid environment and close contact with hard substrates, eventually losing their native structures

and functions. Second, free colloidal suspensions of silver nanoparticles were used for metal-enhanced solution assays.[19-24] Although the solution assay format can provide an aqueous environment for proteins, it is difficult to incorporate this format into miniaturized devices such as microarrays or microfluidic systems that are able to facilitate high-throughput and multiplexed assays.

In this study, as one solution for the problems associated with plate- and particle-based platforms, we developed a novel silver-based MEF biosensing platform that consisted of poly(ethylene glycol)(PEG) hydrogel microstructures entrapping silica-coated AgNPs ($Ag@SiO_2$). Hydrogels are three-dimensional polymeric structures that absorb water or other biological fluids, and therefore have a soft and hydrated nature. Hydrogels are capable of encapsulating proteins, and hydrogel-entrapped proteins can remain structurally intact and maintain their biological function due to the relatively inert aqueous environment within the hydrogel matrix.[25-27] AgNPs were coated with different thickness of silica to optimize the MEF effects. As a model system, the fluorescence detection of glucose by a sequential bienzymatic reaction was chosen. For this analysis, hydrogel microstructures entrapping glucose oxidase (GOX), peroxidase (POD) and $Ag@SiO_2$ were prepared by a simple photopatterning process. We took advantage of the MEF from $Ag@SiO_2$ within the hydrogel microstructures to improve the performance of the fluorescence detection device. After the successful MEF-induced, highly-sensitive detection of glucose using this microarray format, we incorporated the hydrogel microarray into a microfluidic device for potential use in a micro-total-analysis-system (μ-TAS).

Experimental

Chemicals

Poly(ethylene glycol) diacrylate (PEG-DA)(MW 575 Da), the photoinitiator 2-hydroxy-2-methylpropiophenone (HOMPP), 3-(trichlorosilyl)propyl methacrylate (TPM), the silver nitrate ($AgNO_3$), tetraethyl orthosilicate (TEOS), ammonium hydroxide solution (NH_4OH, 28.0~30.0%), glucose oxidase (GOX, from *Aspergillus niger* type II, 50000 unit/g solids), and peroxidase (POD, Type I, from horseradish, 80 unit/mg solid) were purchased from Sigma-Aldrich (Milwaukee, WI, USA), poly(vinylpyrrolidone) (PVP, MW 10,000 Da) was purchased from Junsei Chemical Co.,Ltd. (Tokyo, Japan). Phosphate buffered saline (PBS, 0.1 M, pH 7.4) was purchased from Invitrogen Corp. (Carlsbad, CA, USA).

Preparation of silver nanoparticles

Silver nanoparticles (AgNPs) were prepared by a modified polyol method where PVP was used as reducing agent and protecting agent.[28] Briefly, 0.8 g PVP was dissolved in 80 mL ethanol under vigorous stirring at room temperature. Then, 0.05 g $AgNO_3$ was added into prepared solution with continuous stirring. The suspension was then stirred at room temperature until the $AgNO_3$ was completely dissolved. This solution was heated up to 130 °C at a constant rate of 1 °C/min and the reaction was allowed to proceed for 2 hours. At the end of the reaction, the solution was cooled down to room temperature. The pure silver particles were separated after the addition of a large amount of acetone and subsequent centrifugation at 8000 rpm for 10 minutes. The precipitates, which could be well re-

dispersed in alcohol, were used for subsequent experiments.

Preparation of silica-coated AgNPs ($Ag@SiO_2$)

Silica was directly coated onto the surface of silver nanoparticles through the Stöber method. $Ag@SiO_2$ was prepared by hydrolysis and condensation of TEOS in ethanol using ammonia as catalyst.[21] The 2 mL solution containing silver nanoparticles (2.0 mg/mL) was sonicated for 10 minutes to prevent aggregation. Different amounts of TEOS were added into the solutions of silver nanoparticles under normal stirring. After 10 minutes, 200 μL NH_4OH was added to carry out the silica growth reaction at room temperature under continuous stirring for 8 hours. The $Ag@SiO_2$ was then collected by several centrifugations and re-dispersed in ethanol. Different amounts (0.1, 0.2, 0.3, and 0.5 mL) of TEOS were used in the reaction to control the thickness of the silica shell.

Characterization of nanoparticles

The morphology of the AgNPs and $Ag@SiO_2$ was observed with a Tecnai F12 transmission electron microscope (TEM) operating at an acceleration voltage of 15 kV (Philips Electron Optics, Netherlands). The sizes of nanoparticles were also investigated with dynamic light scattering (DLS, Zetasizer 3000HSA, Malvern Instruments Ltd., Worcestershire, UK). The UV-Vis absorption spectra of AgNPs and $Ag@SiO_2$ were recorded on a Shimadzu 160A Model UV-Vis spectrophotometer (Kyoto, Japan) with a scan range of 200 to 600 nm.

Fabrication of the microfluidic device

The microfluidic networks were formed from a 10:1 mixture of the PDMS pre-polymer and the curing agent as previously described.[29] The resulting mixture was poured onto a silicon master and cured at 60 °C for at least 5 hours. After curing, the PDMS replica was removed from the master and oxidized in oxygen plasma (Femto Science Inc., Seoul, Korea) for 1 minute. Bringing the oxidized PDMS and glass slides into contact resulted in irreversible seals and thus formed enclosed microchannels. To make inlet and outlet ports in the microfluidic device, several holes were punched through PDMS replica using a 16-gauge needle and then connected to a syringe pump (Harvard Apparatus, Holliston, MA, USA) to complete the microfluidic device. The microfluidic devices were mounted onto the stage of a microscope for real-time fluorescence detection and imaging.

Fabrication of hydrogel microarray

Hydrogel microarrays were fabricated by photolithography as reported in our previous studies.[30, 31] After purified PEG-DA was dissolved in PBS to form a 50% w/v solution, 10μL of HOMPP was added to 1 ml of PEG-DA solution to initiate photopolymerization. For the detection of glucose, 1 mg of each enzyme (GOX and POD) was added to 1 mL of precursor solution with or without Ag@SiO_2. The precursor solution was dropped onto glass substrates and covered with a photomask containing microarray patterns. Upon exposure to UV light for 1 second, only exposed regions underwent free-radical-induced gelation and became insoluble. The desired microstructures were obtained by washing away unreacted precursor solution with water so that only the hydrogel microarrays remained

on the substrate surface. The glass surface was modified with TPM to improve the adhesion of the hydrogel microarrays to the surface by creating surface-tethered methacrylate groups capable of covalent bonding with the hydrogel during photopolymerization.[30] When hydrogel microarrays were prepared inside microchannels, the microchannels were filled with precursor solutions and then exposed to UV light for 1 second through a photomask that was aligned on the top of the glass slide. By flushing the channels with PBS, the desired hydrogel structures were obtained inside the microchannels. Figure 1 shows a schematic diagram of the fabrication of the hydrogel microarray entrapping enzymes and Ag@SiO_2.

Fluorescence detection

To analyze the reaction between the enzymes and the glucose fluorescently, the hydrogel microarrays entrapping GOX and POD with Ag@SiO_2 were prepared and reacted with solutions containing Amplex Red and different concentrations of glucose for 5 minutes. As a control experiment, enzyme-entrapping hydrogel microarray containing SiO_2 nanoparticles without AgNP core was used. The reaction between enzymes and glucose was first characterized in an aqueous environment using a QM-1 fluorescence spectrometer (Photon Technologies International, Monmouth, NJ, USA), and the changes in the emission intensity for the enzyme-catalyzed reactions were monitored at 580 nm. The fluorescent response of the microarrays was also studied using a Zeiss Axiovert 200 microscope equipped with an integrated color CCD camera (Carl Zeiss Inc., Thornwood, NY, USA). After the enzymatic reaction, the fluorescence intensities from microarrays were measured using commercially available image analysis software (KS 300, Carl Zeiss Inc.). All of the fluorescence

intensity data were obtained after subtracting the fluorescence intensity value at zero concentration. A minimum of five enzyme assays were performed with each microarray for data acquisition.

Results and discussion

The preparation of core-shell $Ag@SiO_2$ nanocomposites was undertaken in two steps. First, AgNPs were prepared by a high-temperature solvothermal method with ethylene glycol as the solvent and $AgNO_3$ as the silver precursor in the presence of poly(vinylpyrrolidone) (PVP), which generated AgNPs with a diameter of 15~20 nm size, as shown in Figure 2a. Second, the silica shell was coated onto the surface of the AgNPs through the Stöber method. The thickness of the silica layer was controlled by carefully changing the amount of TEOS (Figure 2b). It is well known that the extent of the MEF effect is strongly dependent on the distance between the metal nanoparticles and the fluorescence molecules.[32, 33] When the fluorescence molecules are too close to the metal surface, a strong fluorescence quenching occurs due to the resonant transfer. In contrast, if the distance is too great, SPR coupling becomes less effective, which results in a decrease in the fluorescence intensity. In this study, the coated silica shell acted as a spacer layer to tune the MEF effects. The capability of controlling the thickness of the silica spacer shells was further investigated by DLS measurement. As shown in Figure 2c, the size of $Ag@SiO_2$ increased with the amount of TEOS. Considering the size of AgNPs, the average shell thickness was 6.2, 11.0, 17.5 and 26.1 nm when the amount of TEOS was 0.1, 0.2, 0.3 and 0.5 mL, respectively. The formation of AgNPs and $Ag@SiO_2$ was also confirmed using UV-Vis spectrophotometry. Figure 2d shows that all of the particles have distinct, characteristic absorption peaks at approximately 420 nm, which arises from the surface plasmon absorbance of AgNPs. The intensities of these peaks increase with the thickness of silica shells and red shifts of the absorbance peaks were observed for silica-coated AgNPs due to the increases of the particle size.

In this study, the fluorescent detection of glucose was performed to investigate the potential application of $Ag@SiO_2$ to MEF-based biosensing. Figure 3a shows the consecutive enzyme-catalyzed reactions that occur in the solution containing both glucose and Amplex Red in the presence of GOX and POD. Briefly, glucose reacts with GOX and is converted into gluconolactone and H_2O_2. Next, non-fluorescent Amplex Red reacts with H_2O_2 in the presence of POD to produce highly fluorescent resorufin that has an emission peak at 580 nm. To demonstrate the MEF effect of $Ag@SiO_2$, the GOX-catalyzed reaction with glucose (10 mM) was first characterized in an aqueous environment containing $Ag@SiO_2$ with different silica shell thickness. As shown in Figure 3b, a significant change in the fluorescence intensities compared with control experiment (reaction only with enzymes) was observed as the thickness of the silica shell changes. In the absence of silica shells, the fluorescence intensity decreased due to fluorescence quenching by the resonant energy transfer process discussed earlier. The MEF effect was observed with increasing the thickness of the silica shells and the maximum enhancement was achieved with 17.5±1.55 nm-thick silica shells. The fluorescence enhancement factor (fluorescence intensity with $Ag@SiO_2$ / fluorescence intensity without $Ag@SiO_2$) was approximately 4.6 at this condition. The extent of the fluorescence enhancement decreased with an increase of silica thickness further than 17.5 nm. Next, the effect of $Ag@SiO_2$ concentration on the MEF effect was investigated by varying the concentrations of $Ag@SiO_2$ from 0.05 to 1.0 mg/mL. As shown in Figure 3c, the fluorescence enhancement became greater as the amount of $Ag@SiO_2$ increased, but significant enhancement was not observed when the $Ag@SiO_2$ concentration was more than 0.5 mg/mL. The TEM images in Figure 3d show the different distributions of $Ag@SiO_2$ between the low (0.1 mg/mL) and high concentration (0.5 mg/mL) conditions.

At low concentration, $Ag@SiO_2$ particles were sparsely distributed. Therefore, the MEF effect would not be exerted on many of the fluorescence molecules. On the other hand, at high concentration (more than 0.5 mg/mL), most of space was filled with $Ag@SiO_2$, which means that a higher proportion of the fluorescence molecules would be under the MEF effect. Based on those results, 0.5 mg/mL of $Ag@SiO_2$ nanoparticles with 17.5 nm-thick silica shells were used for the rest of this study.

After the MEF effect was confirmed using $Ag@SiO_2$ in a solution state, hydrogel microarray entrapping $Ag@SiO_2$ as well as GOX and POD were fabricated to detect different concentrations of glucose. Hydrogel microarrays were fabricated by photolithography using the ability of PEG-DA to gel upon exposure to UV light. $Ag@SiO_2$ nanoparticles (0.5 mg/mL) with 17.5 nm-thick silica shells were added into the enzyme (GOX and POD)-containing hydrogel precursor solution and subsequently entrapped within the hydrogel matrix during the UV-induced gelation process. As shown in Figure 4a, a clearly defined array of hydrogel microstructures (100 μm in diameter and 40 μm in height) was successfully fabricated on the substrate, demonstrating that the presence of $Ag@SiO_2$ did not influence to the generation of hydrogel micropatterns via photopatterning process. Figure 4b shows the absorption spectra of hydrogel microarray entrapping enzyme and $Ag@SiO_2$. Broad absorbance from 250 nm to 350 nm was from PEG hydrogel and absorption peaks at approximately 420 nm from the hydrogel-entrapped $Ag@SiO_2$ was still observed, which confirmed the successful entrapment of enzymes and $Ag@SiO_2$ within hydrogel.

Resultant hydrogel microarrays were used for glucose detection using the same mechanism described earlier. Unlike in the solution system, all of the reactions occurred only inside hydrogel. In our previous studies, it was confirmed that the effect of UV

irradiation on the enzyme activity was negligible, and the mesh size of the PEG hydrogel was large enough to allow the diffusion of glucose and Amplex Red into the hydrogel but also small enough to prevent the leaching of the entrapped enzymes from the hydroge.[34, 35] When the solution containing glucose and Amplex Red encounters the hydrogel, Amplex Red and glucose diffuse into the hydrogel. Subsequently, consecutive enzyme-catalyzed reactions produce fluorescent resorufin within each hydrogel microstructures, which emits a strong red fluorescence as shown in Figure 5a. Furthermore, Figure 5b shows that the fluorescence intensity of the hydrogel microarray was nearly identical at each spot, and the fluorescence was almost homogeneous within the single hydrogel microstructure. These results indicate that the concentration of enzymes and $Ag@SiO_2$ within each of the hydrogel microstructures was similar and that the $Ag@SiO_2$ particles were evenly distributed in the hydrogel microstructures. The maximum fluorescence enhancement factor was approximately 4.6 in this experimental condition, which is a very similar value to that from the solution state. This might result from the fact that the hydrogel can provide enzymes and $Ag@SiO_2$ with an aqueous environment similar to the solution state due to its hydrophilicity and capability to absorb the water. Next, the quantitative detection of glucose was carried out by reacting different concentrations of glucose in hydrogel microarrays with $Ag@SiO_2$ and without $Ag@SiO_2$. The fluorescence intensity increased with the glucose concentration, and the fluorescence intensity and sensitivity (the change in signal per change in concentration) were enhanced using $Ag@SiO_2$-entrapped hydrogel microarrays as shown in Figure 5c. According to these experiments, the detection limit for the hydrogel microarrays with $Ag@SiO_2$ and without $Ag@SiO_2$ was approximately 0.5×10^{-4} mM and 1.0×10^{-3} mM, respectively. The fluorescence enhancement factor ranged from 4.1 to 4.9 in

the glucose concentration range of 10^{-3} mM to 1 mM. The selectivity of the glucose sensor was evaluated by comparing the fluorescence signals from glucose in distilled water with that in serum solution containing interfering species such as uric acid and ascorbic acid. The percentages of the interference are from 1.5% to 7.3% at the glucose concentration in the range of 0.01 mM ~ 0.1 mM. To study the reproducibility of the microarray preparation, six different Ag@SiO_2-entrapped hydrogel microarrays were independently prepared and reacted with same concentration of glucose. The relative standard deviation of the biosensor in response to 0.1 mM glucose was less than 6.5% for different microarrays, indicating the good reproducibility of the biosensor. Furthermore, as shown in Figure 5d, the fluorescence intensity could be tuned so that there was a linear correspondence between the fluorescence intensity and the glucose concentration over the physiologically important range of glucose concentrations (1.0 – 10 mM). Glucose biosensor developed in this study was compared with other fluorescence-based glucose sensing system published recently and summarized in Table 1.[36-42] It should be emphasized that our system showed better performance than most of previous systems. Although some systems showed a better limit of detection, those previous works were restricted to solution-based sensing assays without a multiplex sensing capability and reusability.

On the basis of these results, we prepared hydrogel microstructures entrapping GOX and POD with and without Ag@SiO_2 inside different microchannels to study the potential use of this system in a microfluidic-based lab on a chip device that has advantages over the normal microarray system. Using a well-established method to create the microfluidic devices, approximately 200 μm wide and 50 μm deep microchannels were created in PDMS. After the hydrogel microarrays with and without Ag@SiO_2 were fabricated in different

microchannels by a simple photopatterning process as shown in optical image of Figure 6a, the same concentrations of glucose solutions (10 mM) were injected into the microchannels via capillary force and reacted with the hydrogel-entrapped enzymes for 5 minutes. As shown in the fluorescence image of Figure 6a, the hydrogel microarrays in all of the microchannels emitted red fluorescence as a result of the sequential bienzymatic reaction. However, a much stronger fluorescence emission was detected from the hydrogel microarrays with Ag@SiO_2 due to the MEF effects. Figure 6b provides quantitative data showing the change in fluorescence intensity with glucose concentration from hydrogel microarrays with and without Ag@SiO_2 inside the microchannels. A similar fluorescence enhancement factor (4.1~4.7) was observed in the Ag@SiO_2-entrapped hydrogel compared with previous microarray system.

Although MEF effect was solely controlled by the distance between AgNP and fluorescent dye in this study, it was also reported that MEF could be further enhanced not only by controlling the size and shape of metal nanoparticles,[5] but also by the overlap between the absorption spectra of fluorescent dye and the extinction spectra of metal nanoparticles.[43, 44] Therefore, future studies will focus on enhancing the MEF effect by using larger or more anisotropic AgNPs or by tuning the absorption spectra of fluorescent molecules and metal nanoparticles.

Conclusion

In this study, we developed hydrogel microarray systems that can be utilized as an MEF-based biosensing platform. As a model experiment, the fluorescence detection of glucose via a sequential bienzymatic reaction of GOX and POD was performed. A simple

photopatterning process created well-defined hydrogel microarrays entrapping two enzymes without causing their deactivation. $Ag@SiO_2$ nanoparticles were also successfully entrapped within hydrogel micropatterns to exploit the benefits of using silver cores for MEF effects. MEF effects from $Ag@SiO_2$ could be realized by tuning the thickness of the silica shells and the amount of $Ag@SiO_2$ nanoparticles within hydrogel microstructures. At the optimized conditions, a significant improvement in the fluorescence signal and sensitivity of glucose sensing were observed in the presence of $Ag@SiO_2$ nanoparticles due to the MEF effects in comparison with hydrogel microarrays that did not contain the nanoparticles. We also demonstrated that the MEF-inducing hydrogel microarray could be integrated into a microfluidic device for potential use in a micro-total-analysis-system (μ-TAS) as a biosensor. The hydrogel microarray approach described here can be extended to other MEF biosensing platforms, not only for enzyme-based assay but also immunoassays or DNA sensors, by immobilizing antibodies or DNA within hydrogel microarrays.

Acknolowdgements

This work was supported by the Priority Research Centers Programs (2009-0093823) and Active Polymer Center for Pattern Integration at Yonsei University (2007-0056091) through National Research Foundation of Korea (NRF).

References

1. B. Leca-Bouvier and L. J. Blum, *Anal. Lett.*, 2005, **38**, 1491-1517.
2. O. Stoevesandt, M. J. Taussig and M. Y. He, *Expert Rev. Proteomic*, 2009, **6**, 145-157.
3. H. Y. Sun, G. Y. J. Chen and S. Q. Yao, *Chem. Biol.*, 2013, **20**, 685-699.
4. K. Aslan, I. Gryczynski, J. Malicka, E. Matveeva, J. R. Lakowicz and C. D. Geddes, *Curr. Opin. Biotechnol.*, 2005, **16**, 55-62.
5. E. Petryayeva and U. J. Krull, *Anal. Chim. Acta*, 2011, **706**, 8-24.
6. N. Sui, L. N. Wang, T. F. Yan, F. Y. Liu, J. Sui, Y. J. Jiang, J. Wan, M. H. Liu and W. W. Yu, *Sens.Actuator B-Chem.*, 2014, **202**, 1148-1153.
7. M. Bauch, K. Toma, M. Toma, Q. W. Zhang and J. Dostalek, *Plasmonics*, 2014, **9**, 781-799.
8. C. D. Geddes and J. R. Lakowicz, *J. Fluoresc.*, 2002, **12**, 121-129.
9. K. Aslan, J. R. Lakowicz and C. D. Geddes, *J. Phys. Chem. B*, 2005, **109**, 6247-6251.
10. O. Kulakovich, N. Strekal, A. Yaroshevich, S. Maskevich, S. Gaponenko, I. Nabiev, U. Woggon and M. Artemyev, *Nano Lett.*, 2002, **2**, 1449-1452.
11. P. P. Pompa, L. Martiradonna, A. D. Torre, F. D. Sala, L. Manna, M. De Vittorio, F. Calabi, R. Cingolani and R. Rinaldi, *Nat. Nanotechnol.*, 2006, **1**, 126-130.
12. K. Aslan, J. Huang, G. M. Wilson and C. D. Geddes, *J. Am. Chem. Soc.*, 2006, **128**, 4206-4207.
13. C. D. Geddes, H. Cao, I. Gryczynski, Z. Gryczynski, J. Y. Fang and J. R. Lakowicz, *J. Phys. Chem. A*, 2003, **107**, 3443-3449.
14. J. Malicka, I. Gryczynski and J. R. Lakowicz, *Biochem. Biophys. Res. Commun.*, 2003,

306, 213-218.

15. E. G. Matveeva, I. Gryczynski, A. Barnett, Z. Leonenko, J. R. Lakowicz and Z. Gryczynski, *Anal. Biochem.*, 2007, **363**, 239-245.

16. R. Nooney, A. Clifford, X. Leguevel, O. Stranik, C. McDonagh and B. D. Maccraith, *Anal. Bioanal. Chem.*, 2010, **396**, 1127-1134.

17. Y. Wang, Z. Li, H. Li, M. Vuki, D. Xu and H. Y. Chen, *Biosens. Bioelectron.*, 2012, **32**, 76-81.

18. X. Wei, H. Li, Z. Li, M. Vuki, Y. Fan, W. Zhong and D. Xu, *Anal. Bioanal. Chem.*, 2012, **402**, 1057-1063.

19. K. Aslan, J. R. Lakowicz, H. Szmacinski and C. D. Geddes, *J. Fluoresc.*, 2004, **14**, 677-679.

20. K. Aslan, M. Wu, J. R. Lakowicz and C. D. Geddes, *J. Fluoresc.*, 2007, **17**, 127-131.

21. K. Aslan, M. Wu, J. R. Lakowicz and C. D. Geddes, *J. Am. Chem. Soc.*, 2007, **129**, 1524-1525.

22. O. G. Tovmachenko, C. Graf, D. J. van den Heuvel, A. van Blaaderen and H. C. Gerritsen, *Adv. Mater.*, 2006, **18**, 91-95.

23. L. Q. Guo, A. H. Guan, X. L. Lin, C. L. Zhang and G. N. Chen, *Talanta*, 2010, **82**, 1696-1700.

24. P. P. Hu, L. L. Zheng, L. Zhan, J. Y. Li, S. J. Zhen, H. Liu, L. F. Luo, G. F. Xiao and C. Z. Huang, *Anal. Chim. Acta*, 2013, **787**, 239-245.

25. M. Ikami, A. Kawakami, M. Kakuta, Y. Okamoto, N. Kaji, M. Tokeshi and Y. Baba, *Lab Chip*, 2010, **10**, 3335-3340.

26. S. Kiyonaka, K. Sada, I. Yoshimura, S. Shinkai, N. Kato and I. Hamachi, *Nat. Mater.*,

2004, **3**, 58-64.

27. S. Zhang, *Nat. Mater.*, 2004, **3**, 7-8.

28. F. Zhang, G. B. Braun, Y. F. Shi, Y. C. Zhang, X. H. Sun, N. O. Reich, D. Y. Zhao and G. Stucky, *J. Am. Chem. Soc.*, 2010, **132**, 2850-2851.

29. D. C. Duffy, J. C. McDonald, O. J. A. Schueller and G. M. Whitesides, *Anal. Chem.*, 1998, **70**, 4974-4984.

30. A. Revzin, R. J. Russell, V. K. Yadavalli, W. G. Koh, C. Deister, D. D. Hile, M. B. Mellott and M. V. Pishko, *Langmuir*, 2001, **17**, 5440-5447.

31. D. N. Kim, W. Lee and W. G. Koh, *Anal.Chim. Acta*, 2008, **609**, 59-65.

32. K. Ray, R. Badugu and J. R. Lakowicz, *Langmuir*, 2006, **22**, 8374-8378.

33. K. Ray, R. Badugu and J. R. Lakowicz, *Chem. Mater.*, 2007, **19**, 5902-5909.

34. E. Jang and W. G. Koh, *Sens. Actuator B-Chem.*, 2010, **143**, 681-688.

35. W. Lee, D. Choi, J. H. Kim and W. G. Koh, *Biomed. Microdevices*, 2008, **10**, 813-822.

36. S. Cubuk, E. K. Yetimoglu, M. V. Kahraman, P. Demirbilek and M. Firlak, *Sens. Actuator B-Chem.*, 2013, **181**, 187-193.

37. E. Jang, S. Kim and W. G. Koh, *Biosens. Bioelectron.*, 2012, **31**, 529-536.

38. C. H. Liu and W. L. Tseng, *Anal.Chim. Acta*, 2011, **703**, 87-93.

39. J. H. Peng, Y. H. Wang, J. L. Wang, X. Zhou and Z. H. Liu, *Biosens. Bioelectron.*, 2011, **28**, 414-420.

40. Y. X. Piao, D. J. Han, M. R. Azad, M. Park and T. S. Seo, *Biosens. Bioelectron.*, 2015, **65**, 220-225.

41. P. Wu, Y. He, H. F. Wang and X. P. Yan, *Anal. Chem.*, 2010, **82**, 1427-1433.

42. J. Yuan, W. Guo and E. Wang, *Biosens. Bioelectron.*, 2008, **23**, 1567-1571.

43. J. L. Geng, J. Liang, Y. S. Wang, G. G. Gurzadyan and B. Liu, *J. Phys. Chem. B*, 2011, **115**, 3281-3288.

44. Y. S. Wang, B. Liu, A. Mikhailovsky and G. C. Bazan, *Adv. Mater.*, 2010, **22**, 656-659.

Table 1. Comparison of the performance of fluorescence-based glucose sensing.

Detection scheme	Assay system	Detection limit	Reference No.
Fluorescence using Amplex Red	Hydrogels within microfluidic device	6.64 μM	40
Phosphorescence quenching by H_2O_2	Solution-based assay using quantum dot	3.0 μM	41
Fluorescence quenching by H_2O_2	Hydrogel-entrapped quantum dots	50 μM	37
Up-converting fluorescence resonance energy transfer	Solution-based assay using up-converting phosphors	0.043 μM	39
Fluorescence using boronic acid	Photopolymerized sensing membrane	0.27 μM	36
Fluorescence using Amplex Red	Solution-based assay using iron oxide nanoparticle	3.2 μM	38
Fluorescence quenching by benzoquinone	Solution-based assay using quantum dot	0.01 μM	42
Fluorescence using Amplex Red	MEF within hydrogel microarray	0.05 μM	This study

Figure captions

Figure 1. Schematic illustration of the preparation of the hydrogel microarrays entrapping enzymes and Ag@SiO_2

Figure 2. Preparation and characterization of core-shell Ag@SiO_2 nanoparticles. (a) TEM images of AgNPs. (b) TEM images of Ag@SiO_2 with different shell thickness. (Shell thickness was controlled by changing the amount of TEOS.) (c) Size distribution of AgNPs and Ag@SiO_2 obtained by DLS measurement. (d) Absorbance spectra of Ag@SiO_2 with different shell thickness.

Figure 3. MEF-based biosensing for the detection of glucose in the solution state. (a) Scheme of consecutive enzyme-catalyzed reactions that occur in the solution containing both glucose and Amplex Red in the presence of GOX and POD. (b) Effect of silica thickness on the MEF effect. (c) Effect of Ag@SiO_2 concentration on the fluorescence intensity enhancement. (d) TEM images of Ag@SiO_2 with different concentrations (left: 0.1 mg/mL, right: 0.5 mg/mL). Concentration of glucose was 10 mM.

Figure 4. Fabrication of hydrogel microarrays entrapping Ag@SiO_2 and enzymes. (a) SEM images (left: tilted view, right: side view) of hydrogel microarrays. (b) Absorption spectra of hydrogel microarray

Figure 5. Detection of glucose within hydrogel microarray entrapping Ag@SiO_2 and enzymes. (a) Fluorescence image of hydrogel microarrays reacted with glucose (1 mM) and

Amplex Red. (b) Fluorescence intensity profile across the different spots. (c) Comparison of fluorescence intensity between hydrogel microarray with $Ag@SiO_2$ and without $Ag@SiO_2$ at different concentration of glucose. (d) Change of fluorescence intensity within the physiologically important glucose concentration range (1.0 – 10 mM).

Figure 6. Incorporation of $Ag@SiO_2$-entrapped hydrogel microarray into microfluidic system for glucose detection. (a) Optical and fluorescence images of hydrogel microarray with and without $Ag@SiO_2$ after exposure to same concentration of glucose (10 mM) and Amplex Red. (b) Change of fluorescence intensity with glucose concentration from hydrogel microarrays with and without $Ag@SiO_2$ inside microchannels

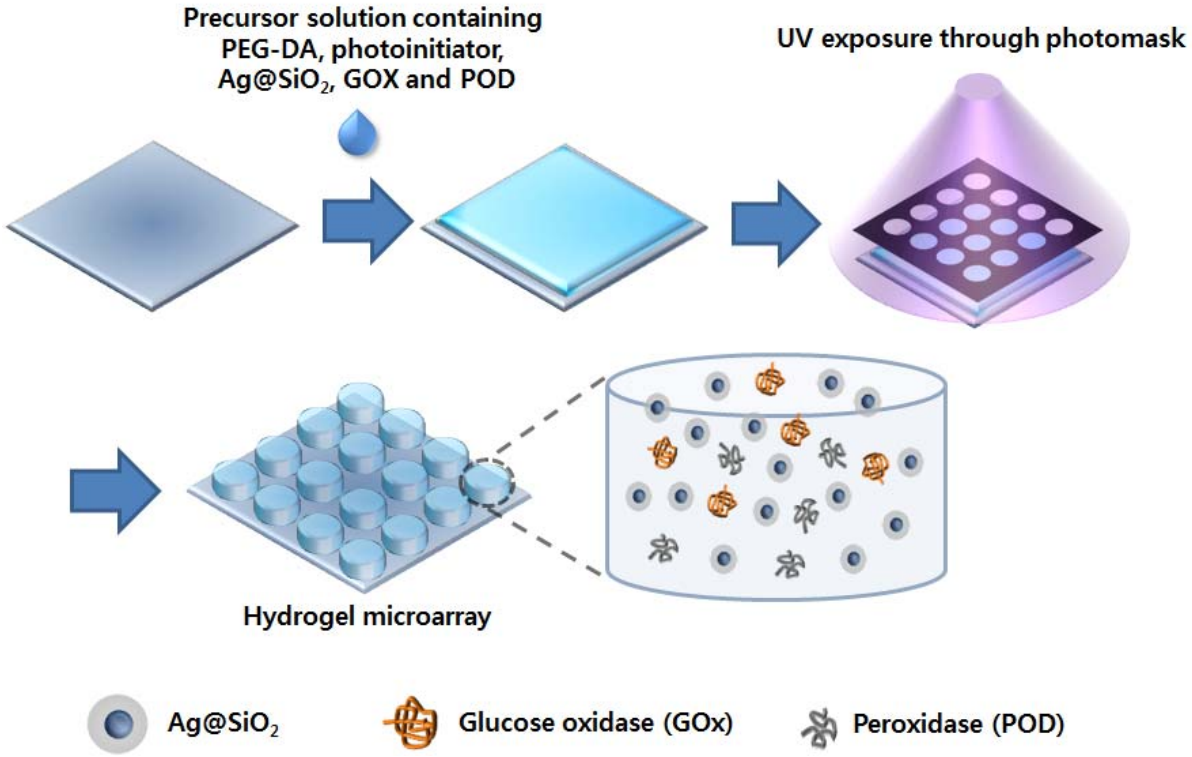

Figure 1. Jang et al.

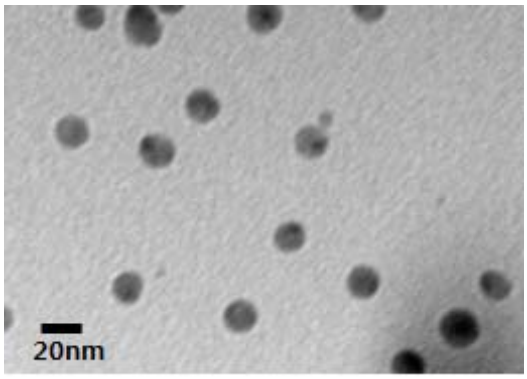

(a)

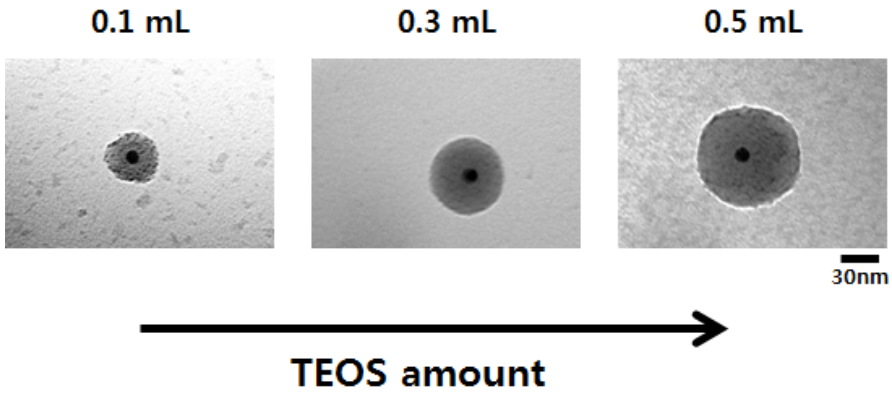

(b)

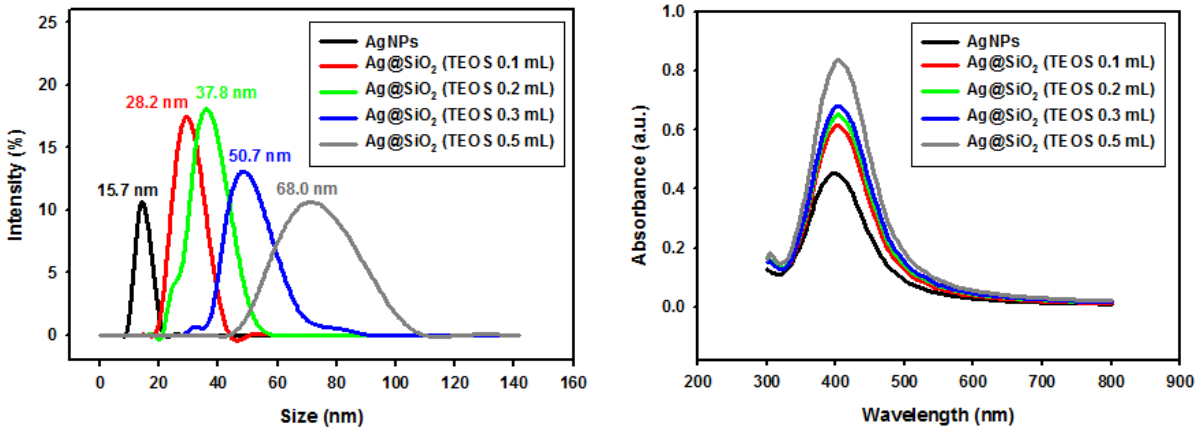

(c) (d)

Figure 2. Jang et al.

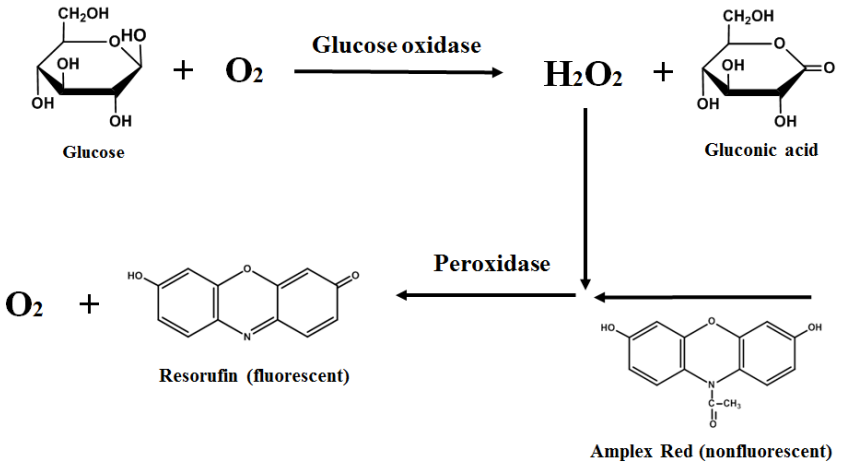

(a)

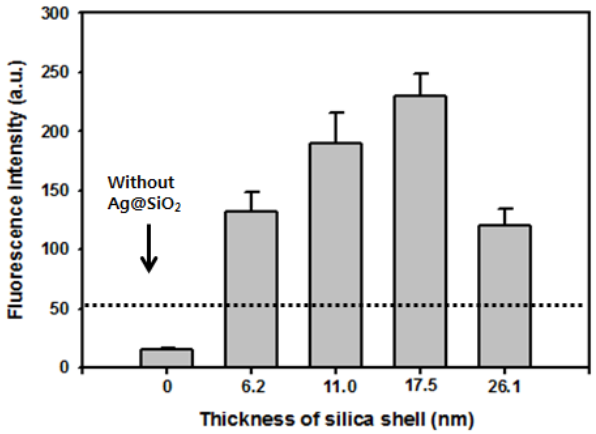

(b)

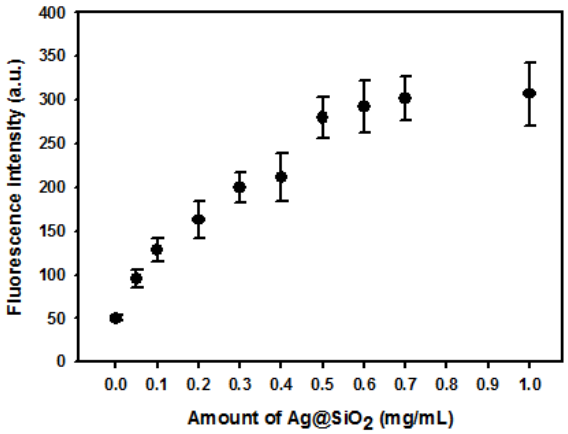

(c)

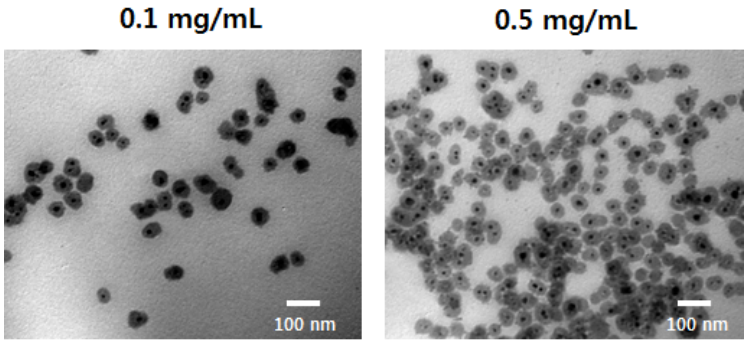

(d)

Figure 3. Jang et al.

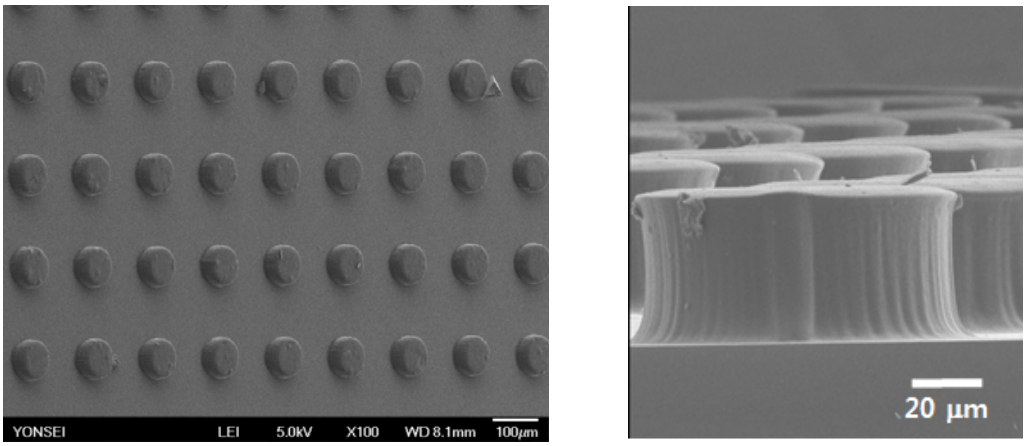

(a)

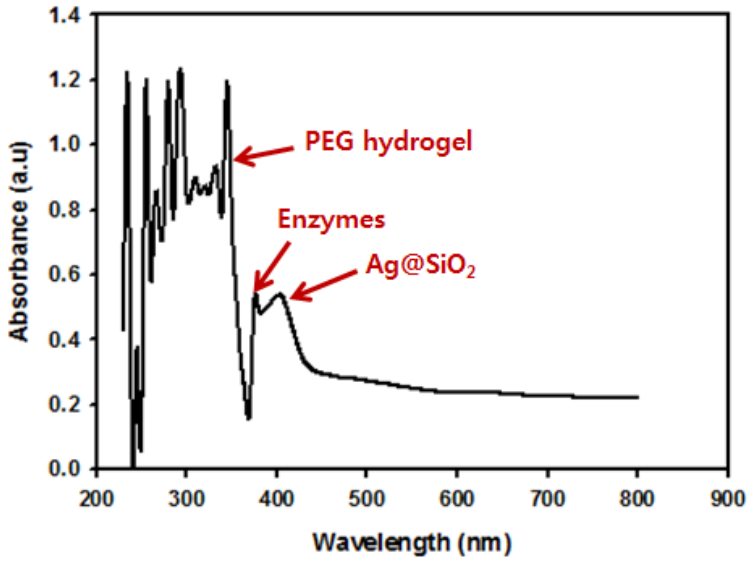

(b)

Figure 4. Jang et al.

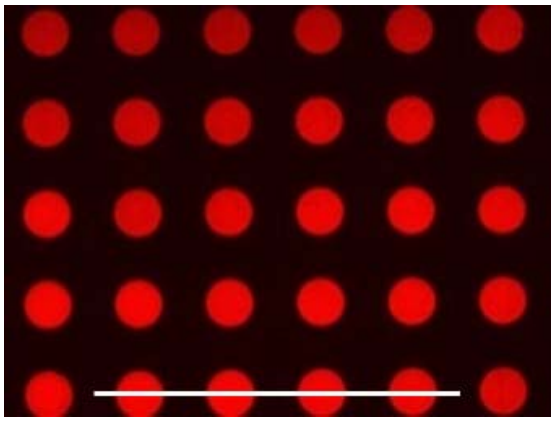

(a)

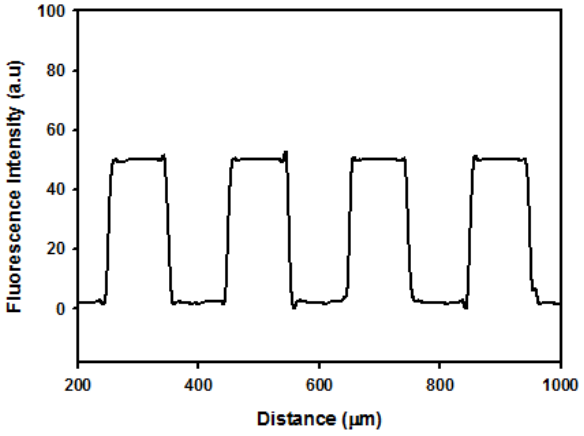

(b)

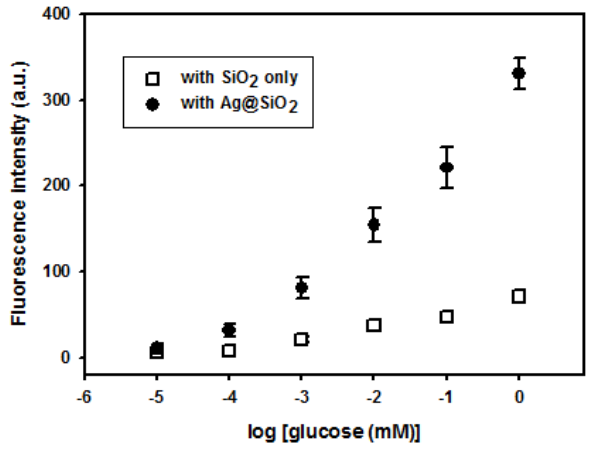

(c)

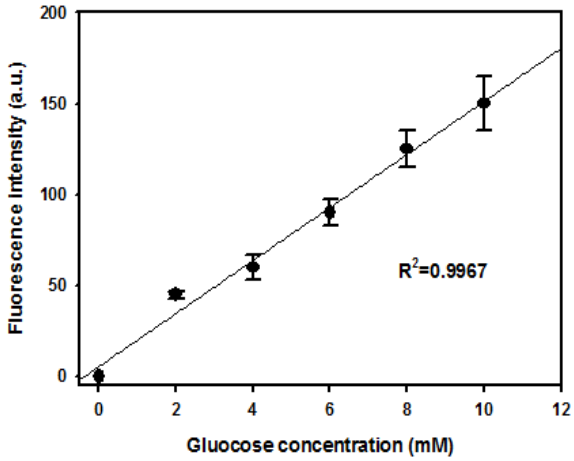

(d)

Figure 5. Jang et al.

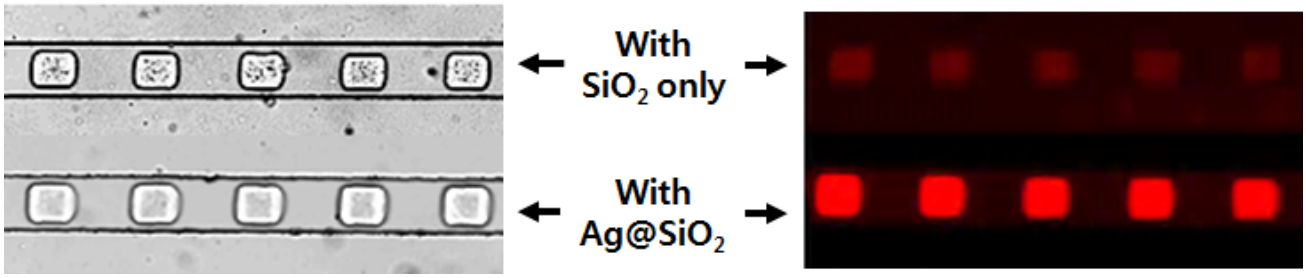

(a)

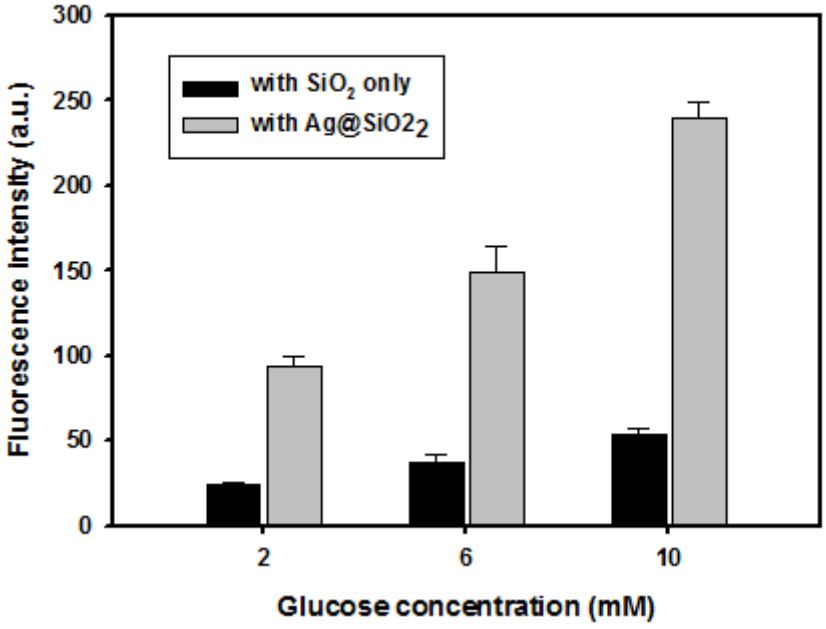

(b)

Figure 6. Jang et al.

We developed novel silver-based metal-enhanced fluorescence (MEF) biosensing platform that consisted of poly(ethylene glycol)(PEG) hydrogel microstructures entrapping silica-coated silver nanoparticles ($Ag@SiO_2$).